Numerical Modelling of Large-Diameter Steel Piles at Horns Rev

Augustesen, Anders Hust; Brødbæk, K. T.; Møller, M.; Sørensen, Søren Peder Hyldal; Ibsen, Lars Bo; Pedersen, Thomas Schmidt; Andersen, Lars

Published in:
Proceedings of the Twelfth International Conference on Civil, Structural and Environmental Engineering Computing

Publication date:
2009

Document Version
Publisher's PDF, also known as Version of record

Paper 239

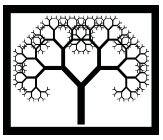

Proceedings of the Twelfth International Conference on Civil, Structural and Environmental Engineering Computing, B.H.V. Topping, L.F. Costa Neves and R.C. Barros, (Editors), Civil-Comp Press, Stirlingshire, Scotland

Numerical Modelling of Large-Diameter Steel Piles at Horns Rev

A.H. Augustesen, K.T. Brødbæk, M. Møller, S.P.H. Sørensen
L.B. Ibsen, T.S. Pedersen and L. Andersen
Department of Civil Engineering
Aalborg University, Denmark

Abstract

Today large-diameter monopiles are the most common foundation type used for large offshore wind farms. This paper aims to investigate the behaviour of monopiles under monotonic loading taking the interaction between the pile and the subsoil into account. Focus is paid to a monopile used as foundation for a wind turbine at Horns Rev located in the Danish sector of the North Sea. The outer diameter of the pile is 4 m and the subsoil at the location consists primarily of sand. The behaviour of the pile is investigated under realistic loading conditions by means of a traditional Winkler-type approach and by means of the commercial three-dimensional numerical program FLAC^{3D}.

Keywords: monopole, *p*-*y* curves, sand, FLAC^{3D}, Winkler approach, API.

1 Introduction

Large-diameter piles are often used as foundations for offshore wind turbines. Such monopiles have diameters around 4–6 m and embedded lengths of 20–30 m depending on the magnitude of the loads and the soil conditions, i.e. the length-diameter ratio is approximately 5.

Monopiles are traditionally designed based on *p*-*y* curves, i.e. a Winkler approach formulating the soil response as uncoupled non-linear springs based on semi-empirical relations between the soil pressure *p* acting against the pile wall and the lateral deflection *y* of the pile, cf. Section 3. For piles in sand, the *p*-*y* curves proposed in design regulations such as [1–3] are based on few full-scale measurements on two steel pipe piles (diameter = 0.61 m, wall thickness = 9.5 mm and embedded length = 21 m) leading to a length–diameter ratio equal to 34.4, as discussed in the work by Cox et al. [4], Reese et al. [5] and O'Neill and Murchinson [6]. The piles have been tested three and four times within a period of approximately two months after installation.

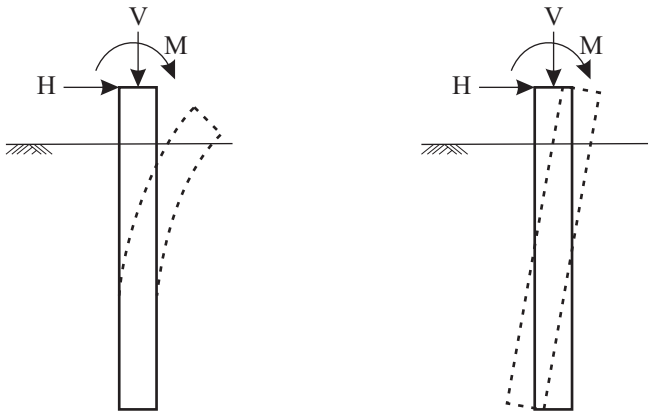

Figure 1: Flexible versus rigid pile behaviour.

Both cyclic and static loading tests were conducted. Further, the proposed *p-y* curves have been tested against a database of lateral pile load tests with satisfaction as described by Murchinson and O'Neill [7]. However, they indicate that the assessment of the *p-y* curves are based on a small database due to the unavailability of appropriately documented full-scale test data.

Briaud et al. [8] postulate that the soil–pile behaviour is affected by the flexibility of the pile, cf. Figure 1. Criteria for rigid or flexible behaviour have been suggested by various researchers, e.g. Poulus and Hull [9]. According to the recommendations proposed by Poulus and Hull [9], the piles used for the development of the *p-y* curves behave as flexible piles. In contrast, the monopile considered in this paper, and generally the monopiles for offshore wind turbines, behave more like rigid piles than flexible ones, i.e. they merely rotate when subjected to large horizontal loads and rocking moments implying a "toe kick", cf. Figure 1. Hence, the deformation behaviour of the piles and thereby the soil in the case of monopiles for nowadays offshore wind turbines is very different from the conditions from which the *p-y* curves are derived. These scale effects have not been taken into account in the currently recommended *p-y* curve formulations [1–3]. Commercial finite element programs such as PLAXIS [10] and ABAQUS [11] as well as the finite difference program FLAC^{3D} [12] do not suffer from these shortcomings. Further, much more complicated models for both soil and pile can be employed leading to a more accurate estimation of the load–deformation behaviour of the pile.

In this paper, results of numerical calculations, conducted by means of FLAC^{3D} [12], of the load–deflection behaviour of a monopile for an offshore wind turbine are presented and compared to the results obtained by means of a traditional Winkler-type approach employing the currently recommended *p-y* curves. The two approaches are compared based on a monopile used as foundation for a wind turbine at Horns Rev located in the Danish sector of the North Sea. Drained conditions and a static load scenario are considered.

2 Horns Rev wind farm

The wind turbine considered is part of Horns Rev Offshore Wind Farm, built during 2003 and located in the North Sea west of Esbjerg in Denmark. The distances to the shore toward the east (Blåvands Huk) and south (Fanø) are approximately 14 km and 28 km, respectively. The farm consists of 80 turbines of the type Vestas V80 with a tower height of 60 m and a rotor diameter of 80 m. The turbines operate at 2 MW, leading to a total amount of installed power of 160 MW. The wind turbines are located in a regular quadrilateral grid and the distances between the turbines in the east-west and north-south directions are 560 m (seven times the rotor diameter) leading to a total park area of approximately 20 km^2. The azimuth for the east-west row is 90° whereas the azimuth for the north-south column is 357° if the reference plane (0° azimuth) is true north.

2.1 Pile conditions

Monopiles of steel are used as foundation for the turbines. In general the outer diameters are 4 m and the lengths are between 30 m and 32.7 m. A transition piece (outer and inner diameter are 4.24 m and 4.15 m, respectively) constitutes the transition from the tower to the monopile.

The steel monopile considered in this paper is the foundation for wind turbine 14, which in the following is denoted M14. The outer diameter is 4 m, the length is 31.6 m and the wall thickness WT, and thereby the bending stiffness E_pI_p, varies along the pile as shown in Figure 2. The monopile has been driven to its final position 31.8 m below the mean sea level (MSL) leading to an embedded depth equal to 21.9 m.

In the ultimate limit state (ULS), the monopile is subjected to the static extreme loads: the horizontal load $H = 4.6$ MN and the bending moment $M = 95$ MNm, both acting at seabed level, whereas the vertical load is $V = 5.0$ MN. Analyses show that the vertical force V has a negligible effect (less than 0.1 %) on the deflection pattern as well as the moments in the pile. Therefore, $V = 0$ is assumed in the following.

2.2 Soil conditions

An extensive test programme, including geotechnical borings, CPTs and triaxial tests, has been conducted to clarify the subsoil profile at the site. The soil profile at the location of M14 consists primarily of sand and it can roughly be divided in six different layers. The first 6.5 m below the seabed is sand, followed by 7.5 m of silty sand. From 14 m to 18.2 m below the seabed, silt/sand including organic material dominates the soil profile. Hereunder, sand is found.

The soil conditions are summarized in Table 1, where γ and γ' are the unit weight and the submerged unit weight of the soil, respectively, whereas φ is the angle of internal friction and ψ is the dilation angle. The friction angle φ is determined from CPTs according to the procedure proposed by Schmertmann [13]. Apart from the silt/sand layer with organic material all other layers have relatively high angles of internal friction ($36.6° < \varphi < 45.4°$). Further, it is assumed that $\psi = \varphi - 30°$.

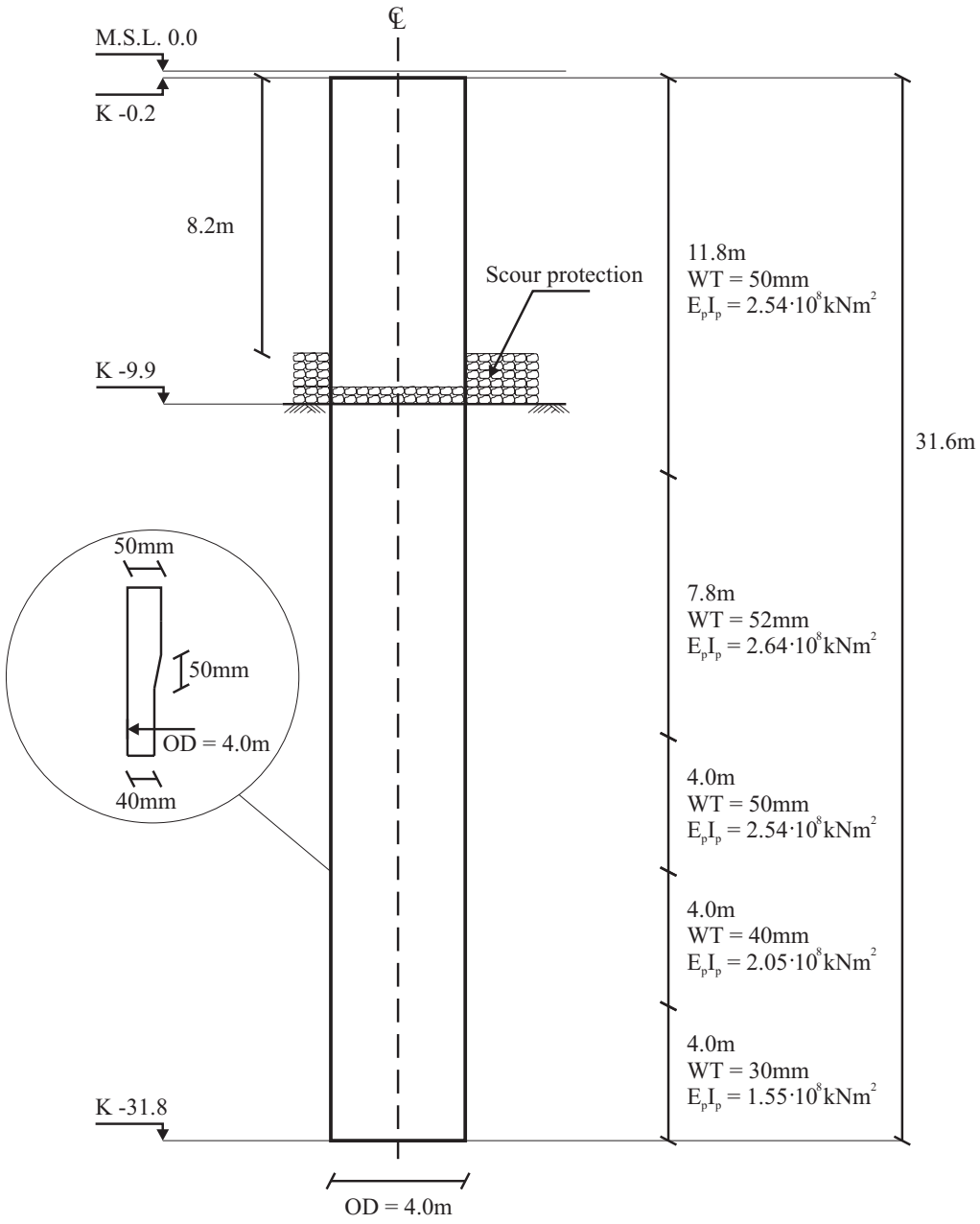

Figure 2: Details of the pile.

The classical Mohr-Coulomb criterion and a linear elastic material model have been combined to describe the elasto-plastic material behaviour of the soil in the numerical calculations, cf. Section 4. In this model, only one stiffness modulus is needed. It is assumed that the stiffness of the soil can be represented by the secant Young's modulus E_s corresponding to an average axial strain of 0.1 % as well as Poisson's ratio v. According to Lunne et al. [14], this level of strain is reasonably representative for many well-designed foundations. E_s is stress-dependent and it is determined according to Lengkeek [15]. Apart from the silt/sand layer with organic material, all soil layers have relatively high stiffness (100 MPa < E_s < 168.8 MPa).

Soil layer	Type	Depth [m]	E_s [MPa]	γ / γ' [kN/m3]	φ [°]	ψ [°]	ν [-]
1	Sand	0 - 4.5	130	20/10	45.4	15.4	0.28
2	Sand	4.5 - 6.5	114.3	20/10	40.7	10.7	0.28
3	Sand to silty sand	6.5 - 11.9	100	20/10	38.0	8	0.28
4	Sand to silty sand	11.9 - 14.0	104.5	20/10	36.6	6.6	0.28
5	Sand/silt/organic	14.0 - 18.2	4.5	17/7	27.0	0	0.28
6	Sand	18.2 →	168.8	20/10	38.7	8.7	0.28

Table 1: Soil profile including average values of the strength and stiffness parameters for each soil layer.

3 Winkler model—the API method

Laterally loaded monopiles used for wind turbine foundations are traditionally designed based on a Winkler approach [16], i.e. a beam supported by an elastic foundation representing the soil. Thus, the soil is assumed to consist of continuously distributed disjoint horizontal springs. In contrast to a Pasternak foundation, the soil has no shear stiffness but only lateral stiffness, represented by nonlinear elastic springs based on semi-empirical relations between the soil pressure p acting against the pile wall and the lateral deflection y of the pile, cf. Figure 3. The spring stiffness E_{py}, normally denoted the modulus of subgrade reaction, is provided by the p-y curves as the secant modulus, cf. Figure 3. Generally, E_{py} increases with depth x and decreases with increasing deflections y. Further, E_{py} depends on the soil conditions, and in the static loading case, the p-y curves reach a horizontal asymptote corresponding to the capacity of the soil p_{ult}. If not measured at a given site, the p-y curves provided by current design regulations, such as the American Petroleum Institute (API) [1] and Det Norske Veritas, [2–3], can be employed. A consistent review of p-y curves for piles in cohesionless soil is presented by Brødbæk et al. [17].

Based on the Winkler approach, the governing differential equation describing the horizontal deflection of a pile subjected to the horizontal load H and the bending moment M is given by:

$$E_p I_p \frac{d^4 y}{dx^4} - E_{py} y = 0\,, \tag{1}$$

where y is the lateral deflection of the pile at a point x along the pile, E_pI_p is the bending stiffness, or flexural stiffness, of the pile with E_p denoting Young's modulus, and I_p is the second moment of area around a horizontal axis perpendicular to the pile axis. For the studied monopile E_pI_p changes with depth as shown in Figure 2. A traditional sign convention has been employed. However, the soil pressure p is assumed positive in the direction opposite to the displacements y and the applied horizontal force H.

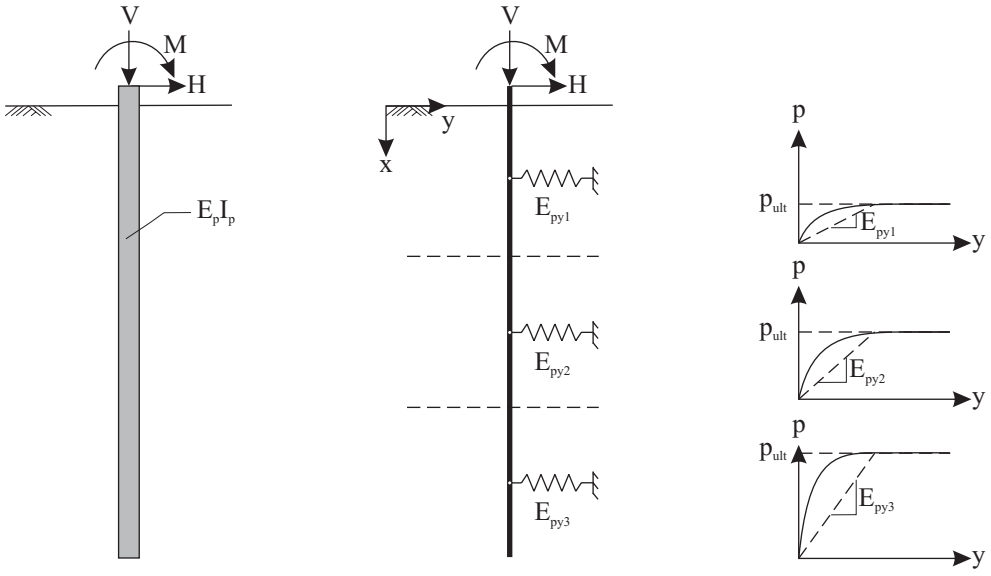

Figure 3: Winkler approach and definition of *p-y* curves.

The pile is modelled as a Bernoulli-Euler beam in spite of its relatively small length–diameter ratio. In principle, the Timoshenko beam theory [18] could preferably be applied. However, in practice the Bernoulli-Euler beam theory suffices since the pile is very stiff, behaving more like a rigid pile than a flexible one, cf. Sections 1 and 5.

The *p-y* curves presented in Section 2.1, and recommended by API [1], are based on tests on piles located in almost homogeneous soil. The soil profile at Horns Rev is layered but sand dominates as described in Section 2. Therefore, the procedure of Georgiadis [19], which accounts for layered soil within the framework of the *p-y* curve method, has been employed. The method is based on the estimation of an equivalent depth of all the soil layers existing below the upper layer. Based on these equivalent depths, the *p-y* curve for a layer is determined as if the soil is homogeneous and the top of the layer in consideration is located at a depth corresponding to the equivalent depth of the layer. Hence, the *p-y* curve formulations described in Section 2.1 can be applied unaltered. However, instead of using the real depth for the top of each layer in the formulations, the equivalent depth of the top of each layer is employed.

In this study, Equation (1) has been solved under the auspices of the finite element method by introducing appropriate boundary conditions. It turns out that the solution converges if approximately 100 elements are used. The Winkler approach based on the *p-y* curves proposed by API [1] will, in the following, be referred to as the *API method*.

3.1 *p-y* curves for piles in sand

According to API [1], the *p-y* relationship for piles in sand is given by

$$p = A \cdot p_{\text{ult}} \tanh\left(\frac{k_{\text{sand}} \cdot x \cdot y}{A \cdot p_{\text{ult}}} \right) \tag{2}$$

p_{ult} is the ultimate lateral resistance at depth x below the surface, k_{sand} is the initial modulus of subgrade reaction, y is the lateral deflection, D is the average pile diameter and A is a factor accounting for cyclic or static loading conditions; $A = 0.9$ for cyclic loading and $A = (3.0 - 0.8\, x/D) \geq 0.9$ for static loading. k_{sand} depends on the angle of internal friction φ. An expression for k_{sand} has been fitted based on [1]:

$$k_{\text{sand}} = \left(0.008085 \cdot \varphi^{2.45} - 26.09\right) \cdot 10^3 \quad \text{[kPa/m]}, \quad 29° \leq \varphi \leq 45° . \tag{3}$$

The lateral capacity p_{ult} varies from a value at shallow depths,

$$p_{\text{ult,shallow}} = \left(C_1 \cdot x + C_2 \cdot D\right) \cdot \sigma_v , \tag{4}$$

to a value at deep depths,

$$p_{\text{ult,deep}} = C_3 \cdot D \cdot \sigma_v , \tag{5}$$

where σ_{v} is the effective overburden pressure at the considered depth. At a given depth the equation giving the smaller value of p_{ult} should be used as the capacity. The coefficients C_1, C_2 and C_3 are functions of φ and can be determined from [1]. However, they can alternatively be described by the following expressions [20]:

$$C_1 = 0.115 \cdot 10^{0.0405 \cdot \varphi}, \quad C_2 = 0.571 \cdot 10^{0.022 \cdot \varphi}, \quad C_3 = 0.646 \cdot 10^{0.0555 \cdot \varphi} . \tag{5}$$

4 FLAC^{3D} model

A three-dimensional numerical model has been established to investigate the displacement of the pile during horizontal loading. The computations are carried out by means of FLAC^{3D} [12], which is a three-dimensional, dynamic, explicit finite-difference solver. Due to the symmetry, only one half of the pile and the surrounding soil is considered. The model has an outer diameter of $40D = 160$ m based on the recommendations by Abbas et al. [21], and the boundary at the bottom is placed approximately 18 m below the pile toe. A view of the model is shown in Figure 4.

The external load in the model is applied as a horizontal force of $H = 2.3$ MN (= 0.5·4.6 MN due to the symmetry) acting at the height $h = 20.65$ m above seabed level. This combination of the height and horizontal force provides a bending moment of $M = 95$ MNm at seabed level, corresponding to the design criterion for the prototype, cf. Section 2.

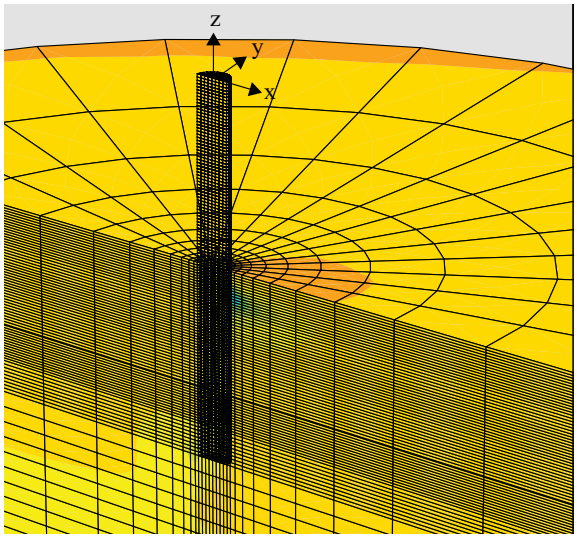

Figure 4: FLAC^{3D} model.

For both the soil and pile, zone elements are used to model the geometry. Each zone consists of five first-order, constant-rate-of-strain, tetrahedral subelements. The monopile is assumed to be linear elastic steel with the parameters E_p = 210 GPa and ν = 0.3. However, the pile is modelled as a solid cylinder rather than an open tubular pile with an internal soil plug. Young's modulus is reduced so that the bending stiffness E_pI_p corresponds to that of M14, cf. Figure 2. Thus, for the equivalent solid pile, E_p is within the range 12.3 GPa to 21.0 GPa. Poisson's ratio is unaltered, since the value for the soil is close to that of steel, cf. Table 1. It should be noted that the shear stiffness of the pile is incorrectly scaled, but it has been found that the shear deformations of the pile have a negligible influence on the overall response of the pile and soil. Similarly to the stiffness, the weight of the solid monopile is adjusted in such way that it corresponds to that of M14. Here, it is assumed that the real, open-ended tubular pile behaves in a plugged way, assuming that the soil inside the pile is located at seabed level.

The materiel behaviour of the soil is modelled using the classical elasto-plastic Mohr-Coulomb model. The employed materiel properties are given in Table 1. The interaction between the monopile and the soil is modelled using a standard FLAC^{3D} interface. A linear Coulomb shear-strength criterion is employed for the interface to limit the shear forces acting at the interface nodes. The interface elements allow gapping and slipping between the soil and the pile.

The finite-difference calculations are executed stepwise. First, the initial stress state is established in the entire model using the submerged unit weight for both the soil elements and the elements that later become the pile. A K_0-procedure, in which it is assumed that $K_0 = 1 - \sin\varphi$, is employed to establish the initial horizontal effective stresses. Subsequently the pile is generated by replacing the soil elements that now become the pile with the adjusted strength and stiffness parameters as well as the adjusted weight corresponding to the monopile for M14. Further, the monopile elements are extended above the ground surface in order to realize the

loading conditions described above. Between the pile elements and the soil elements, an interface is established to model the pile–soil interaction. The system is brought to equilibrium. Finally, the horizontal load is applied incrementally and new equilibrium states are calculated. Damping is introduced in the system to provide a quasi-static solution. Further, different types of grids have been employed to assure convergence, which has been achieved with the grid shown in Figure 4.

5 Results

In Figure 5, the deflections of the monopile for M14 are shown in the case the pile is subjected to the static extreme loads presented in Section 2.1. The monopile behaves relatively rigid implying that a "toe kick" occurs; this is especially pronounced when considering the deflection behaviour predicted by the FLAC^{3D} model. The maximum horizontal deflections determined by means of the API method and FLAC^{3D} are 26.8 mm and 43.5 mm, respectively, i.e. FLAC^{3D} predicts 62 % greater deflections at seabed level compared to the API method, cf. Table 2. Below 14 m the deflection pattern estimated by the API method and FLAC^{3D} deviate significantly. FLAC^{3D} estimates, for example, greater horizontal deflections at the pile toe compared to the API method, cf. Table 2. The deviation in deflection pattern may be due to the fact that the stiffness E_{py} provided by the *p-y* curves is overestimated at great depths, which is also documented by Sørensen et al. [22] as well as Lesny and Wiemann [23]. Since the API method overestimates the stiffness with depth compared to FLAC^{3D}, the depth for zero deflection predicted by the API method is located closer to the seabed, cf. Table 2. Further, the accumulated rotation at seabed level deviates 19 %, with FLAC^{3D} giving rise to a rotation of 0.31° and the API method providing a rotation of 0.26°.

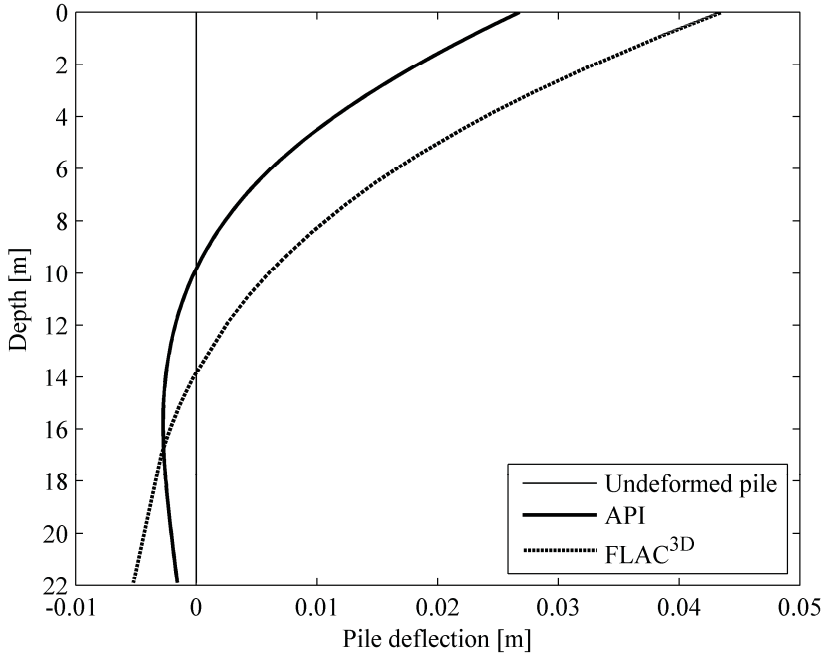

Figure 5: Pile deflections at maximum horizontal load.

	API	FLAC^{3D}	Deviation [%]
Maximum moment [MNm]	105.4	105.4	0
Depth to maximum moment [m]	3.4	2.1	-38
Horizontal deflection at seabed [mm]	26.8	43.5	62
Horizontal deflection at pile toe [mm]	-1.6	-5.2	225
Rotation at seabed [°]	0.26	0.31	19
Depth for zero deflection [m]	9.9	14	-41

Table 2: Results obtained by means of FLAC^{3D} and the API method.

Figure 6 shows the moments in the pile. FLAC^{3D} and the API method predict similar patterns of the moment with depth. However, some deviations in magnitude are observed from 10 m below the seabed. The maximum moments determined by the two approaches are in both cases 105.4 MNm, cf. Table 2. Further, the depths to the maximum moment are 3.4 m and 2.1 m, respectively, with FLAC^{3D} giving rise to the latter value.

The *p-y* curves at different depths are shown in Figure 7. In connection with FLAC^{3D}, the soil pressures *p* acting against the pile wall are estimated by double differentiation of the moment distribution in the pile according to Bernoulli-Euler beam theory. However, double differentiation of discrete signals results in some errors. In order to minimise these errors, the piecewise polynomial curve fitting method proposed by Yang and Liang [24] has been employed. Figure 7 shows that the pressures, estimated by means of FLAC^{3D}, mobilised at the depth x = 7.4 m are

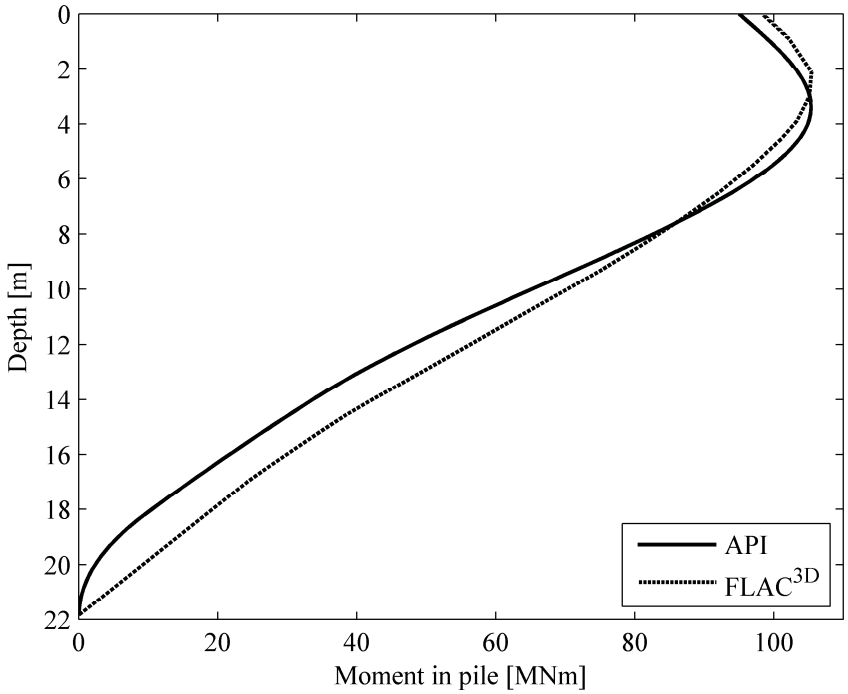

Figure 6: Moments in the pile at maximum loads.

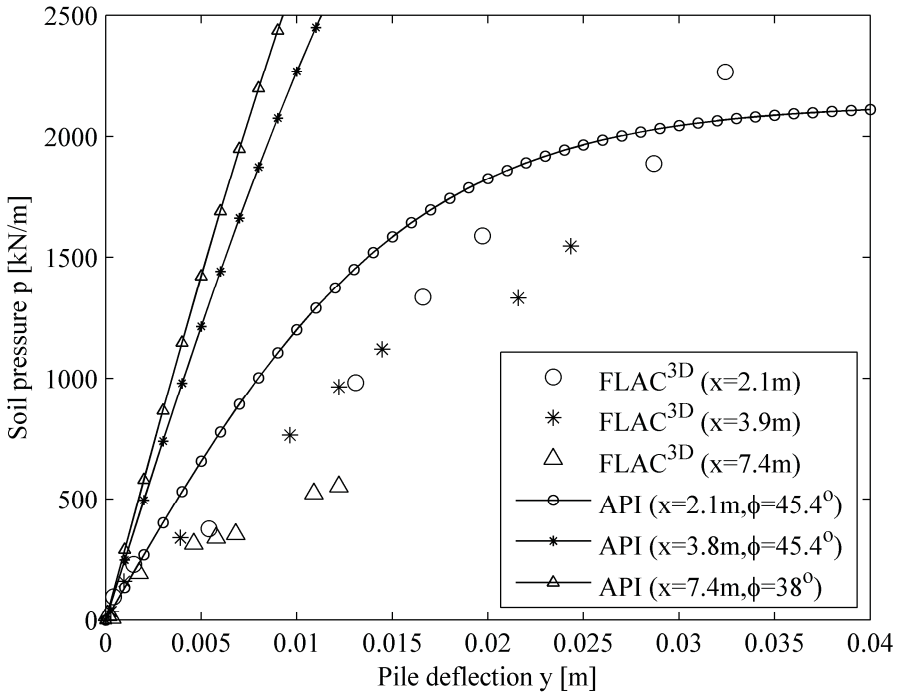

Figure 7: Soil pressures p as function of deflection y and depth x.

less than the pressures at both $x = 2.1$ m and $x = 3.9$ m for a given deflection y. This is due to the lower angle of internal friction of layer 3 compared to layer 1, cf. Table 1. At the depth $x = 2.1$ m there is a relatively good agreement between the predictions by FLAC^{3D} and the API method. However, at greater depths, $x = 3.9$ m and $x = 7.4$ m, the API method significantly overestimates the soil pressures compared to FLAC^{3D}. Further, the initial stiffness

$$E_{\text{py,ini}} = \frac{\partial}{\partial x}\left[A \cdot p_{\text{ult}} \tanh\left(\frac{k_{\text{sand}} \cdot x \cdot y}{A \cdot p_{\text{ult}}} \right) \right]\Bigg|_{y=0} = k_{\text{sand}} \cdot x \tag{6}$$

of the p-y curve at $x = 7.4$ m is slightly higher than $E_{\text{py,ini}}$ for $x = 3.8$ m even though the angle of internal friction of layer 3 is lower compared to layer 1, i.e. the depth compensate for the differences in k_{sand} and thereby φ. Since there is concordance between the results obtained by the API method and FLAC^{3D} for layer 1 ($x = 2.1$ m) but not at the other depths, it can be insinuated that the p-y curves overestimate the stiffness of sand and/or there are some shortcomings in the method proposed by Georgiadis [19], in which layered soil profiles are taken into account under the auspices of the API method. However, Sørensen et al. [22] as well as Lesny and Wiemann [23] document that the stiffness of the p-y curves are, in general, significantly overestimated with depth.

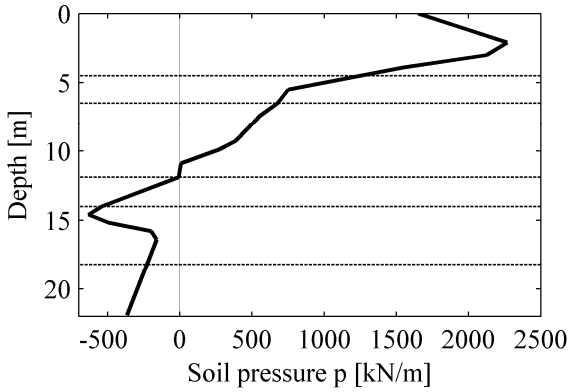

Figure 8: Soil pressures (solid line) along the pile. The transition from one layer to another is marked with dotted lines.

The soil pressure, determined by means of FLAC^{3D}, acting against the pile wall when H = 4.6 MN and M = 95 MNm, is shown in Figure 8. The pressure distribution with depth reflects the tendencies in the pile deflection pattern (Figure 5) as well as the strength of the different layers (Table 1), i.e. the higher deflection and angle of internal friction, the higher the soil pressure. Below the point of zero deflection, the soil pressures change sign corresponding to negative deflections as shown in Figure 5. The depth of zero deflection (Table 2) does not coincide with the depth of zero soil pressure (Figure 8). Further, the soil pressure at seabed is not equal to zero. This indicates that some uncertainties are associated with the way the soil pressures, by double differentiation of the moment distribution in the pile, are estimated.

6 Conclusions

The behaviour of a monopile used as foundation for a wind turbine at Horns Rev located in the Danish sector of the North Sea has been investigated. The outer diameter is 4 m, whereas the embedded length is approximately 22 m. The pile is located primarily in sand and it has been subjected to static extreme loads. The paper presents the results of numerical calculations conducted by means of the commercial three-dimensional finite difference code FLAC^{3D}. These results are compared to the results obtained by means of a traditional Winkler-type approach employing *p-y* curves as proposed in current design regulations for offshore wind turbines. The classical Mohr-Coulomb model based on soil parameters derived from Cone Penetration Tests has been employed to model the soil in FLAC^{3D}.

It can be concluded that the monopile behaves as a relatively rigid pile, implying that only one point of zero deflection exists. The deflections at seabed level and at the pile toe, determined by means of FLAC^{3D}, are 62 % and 225 % greater, respectively, compared to the deflections predicted by a Winkler approach. The total deflections estimated by FLAC^{3D} and the Winkler model at sea bed level are 43.5 mm and 26.8 mm, respectively. Further, the accumulated rotations at seabed level predicted by the two approaches are 0.31° and 0.26°, respectively, with

FLAC^{3D} giving rise to the latter value. In contrast, the maximum moments in the pile predicted by FLAC^{3D} and the Winkler approach are equal.

The Winkler approach is, compared to FLAC^{3D}, generally non-conservative in terms of determining deflections of non-slender large-diameter piles for wind turbines. The reason is that the *p-y* curves for piles in sand significantly overestimate the stiffness of the soil, especially at large depth. Moreover, extreme care should be taken in the estimation of the soil stiffness associated with the constitutive soil models employed in commercial programs such as FLAC^{3D}. Further research is needed to develop new *p-y* curves for large-diameter piles in sand and to verify the conclusions drawn in this paper.

Acknowledgement

The work presented in this paper is partly funded by PSO-F&U 2005 Design of offshore wind turbines (FU5101, Energistyrelsens j.nr.; 79030-0019, PSO-05).

References

[1] API, "RP2A-WSD: Recommended Practice for Planning, Designing and Constructing Fixed Offshore Platforms – Working Stress Design", American Petroleum Institute, 20th edition, 1993.

[2] DNV, "Foundations, Classifications Notes No. 30.4", Det Norske Veritas Classification A/S, Veritasveien 1, 1322 Høvik, Norway, 1992.

[3] DNV, "Offshore Standard DNV-OS-J101: Design of Offshore Wind Turbine Structures", Technical Report DNV-OS-J101, Det Norske Veritas, 2004.

[4] W.R. Cox, L.C. Reese, B.R. Grubbs, "Field Testing of Laterally Loaded Piles in Sand", in "Proceedings of the 6th Annual Offshore Technology Conference", OTC 2079, 459–472, Houston, Texas, USA, 1974.

[5] L.C. Reese, W.R. Cox, F.D. Koop, "Analysis of Laterally Loaded Piles in Sand", in "Proceedings of the 6th Annual Offshore Technology Conference", OTC 2080, 473–484, Houston, Texas, USA, 1974.

[6] M.W. O'Neill, J.M. Murchinson, "An Evaluation of *p-y* Relationships in Sand", a report to the American Petroleum Institute, 1983.

[7] J.M. Murchinson, M.W. O'Neill, "Evaluation of *p-y* Relationships in Cohesionless Soil", in "Analysis and Design of Pile Foundations. Proceedings of a Symposium in Conjunction with the ASCE National Convention", ASCE, 174–191, 1984.

[8] J.L. Briaud, T.D. Smith, B.J. Meyer, "Using Pressuremeter Curve to Design Laterally Loaded Piles", in "Proceedings of the 15th Annual Offshore Technology Conference", OTC 4501, 495–502, Houston, Texas, USA, 1984.

[9] H. Poulus, T. Hull, "The Role of Analytical Geomechanics in Foundation Engineering", in "Foundation Engineering: Current Principles and Practices", 2, 1578–1606, 1989.

[10] R.B.J. Brinkgreve and W. Broere (edt.), PLAXIS 3D Foundation - Manual, The Netherlands, 2006.

[11] ABAQUS Version 6.8, Dassault Systèmes Simulia Corp, Providence, Rhode Island, USA, 2008.
[12] FLAC^{3D} Version 3.1, Itasca Consulting Group Inc., Minneapolis, Minnesota, USA, 2006.
[13] J.H. Schmertmann, "Guidelines for Cone Penetration Test, Performance and Design", Report, FHWA-TS-78-209, 145, US Federal Highway Administration, Washington, DC, 1978.
[14] T. Lunne, P.K: Robertson, J.J.M. Powell, "Cone Penetration Testing in Geotechnical Practice", Blackie Academic & Professional, 1997.
[15] Lengkeek H.J, "Estimation of Sand Stiffness Parameters from Cone Resistance", PLAXIS Bulletin No. 13, 15–19 January, 2003.
[16] E. Winkler, "Die Lehre von Elasticzitat und Festigkeit (on Elasticity and Fixity)", Prague, 1867.
[17] K.T. Brødbæk, M. Møller, S.P.H. Sørensen, A.H. Augustesen, "Review of *p-y* Relationships in Cohesionless Soil", DCE Technical Reports, 57, Department of Civil Engineering, Aalborg University, Aalborg, 2009.
[18] S.P. Timoshenko, "Strength of Materials, Part II, Advanced Theory and Problems", 2nd edition, 10th printing, New York, 1941.
[19] M. Georgiadis, "Development of *p-y* Curves for Layered Soils", in "Proceedings of the Conference on Geotechnical Practice in Offshore Engineering", 536–545, 1983.
[20] PYGMY, "User Manual – Program PYGMY, version 2.3.1", the University of Western Australia, Department of Civil and Resource Engineering, 2000.
[21] J.M. Abbas, Z.H. Chik, M.R. Taha, "Single Pile Simulation and Analysis Subjected to Lateral Load", Electronic Journal of Geotechnical Engineering, 13E, 1–15, 2008.
[22] S.P.H. Sørensen, K.T. Brødbæk, M. Møller, A.H. Augustesen, L.B. Ibsen, "Evaluation of Load–Displacement Relationships for Large-Diameter Piles in Sand", in "Proceedings of the Twelfth International Conference on Civil, Structural and Environmental Engineering Computing", Portugal, 2009.
[23] K. Lesny, J. Wiemann, "Finite-Element-Modelling of Large Diameter Monopiles for Offshore Wind Energy Converters", in "Geo Congress 2006", February 26 to March 1, Atlanta, GA, USA, 2006.
[24] K. Yang, R. Liang, "Methods for Deriving *p-y* Curves from Instrumented Lateral Load Tests", Geotechnical Testing Journal, 30(1), Paper ID GTJ100317, 2006.